Journal of Structural Geology, Vol. 8, No. 8, pp. 831 to 843, 1986
Printed in Great Britain

0191-8141/86 $03.00 + 0.00

Porphyroclast systems as kinematic indicators

C. W. PASSCHIER

Instituut voor aardwetenschappen, Rijksuniversiteit Utrecht, Utrecht 3508 TA, The Netherlands

and

C. SIMPSON

Department of Geological Sciences, Virginia Polytechnic Institute and State University, Blacksburg, VA, 24061, U.S.A.

(*Received* 10 *October* 1985; *accepted in revised form* 18 *March* 1986)

Abstract—Porphyroclasts of relatively strong minerals in mylonites commonly have an internal monoclinic shape symmetry defined by tails of dynamically recrystallized material. The geometry of a porphyroclast and its tails, called a 'porphyroclast system', can serve as a valuable indicator of the sense of vorticity. Porphyroclast systems have been divided into σ- and δ-types on the basis of the geometry of the tails. σ-Types have wedge-shaped recrystallized tails whose median lines lie on opposite sides of a reference plane parallel to the tails and containing the symmetry axis for the system. σ-Types are further subdivided into a σ_a-types, in which the porphyroclast is isolated in a relatively homogeneous matrix, and σ_b-types, in which the porphyroclast system is associated with a shear band foliation in the matrix. δ-Types typically have narrow recrystallized tails whose median lines cross the reference plane adjacent to the porphyroclast. Consequently, embayments of matrix material occur adjacent to the porphyroclasts and the tails display characteristic bends.

A porphyroclast system in a mylonite develops when the relatively weak dynamically recrystallized grain aggregate in the porphyroclast mantle changes its shape due to non-coaxial flow in the adjacent matrix. This behaviour has been modelled in shear box experiments. Passive marker lines around rigid cylinders embedded in silicone putty were subjected to simple shear. The experiments were modified to simulate a change in recrystallization rate ($\dot{R}$) with respect to rate of deformation ($\dot{\gamma}$) by decreasing the diameter of the rigid cylinder during deformation at variable rates. The ratio $\dot{R}/\dot{\gamma}$ appears to be one of the most important factors in determining which porphyroclast system will develop. At high $\dot{R}/\dot{\gamma}$ values, flow of recrystallized material away from the porphyroclast is continuously appended by the production of new grains and wedge-shaped σ_a-type tails develop. At low $\dot{R}/\dot{\gamma}$ values, relatively few new grains are added to the tails which become thinned and deflected by drag due to the spinning motion of the porphyroclast. In addition, most porphyroclast systems at low shear strains are of σ_a-type or lack monoclinic symmetry, whereas δ-types are only developed at high shear strain values. Complex porphyroclast systems, characterized by two generations of tails, are observed in many of the natural and model shear zones studied and may form due to fluctuating $\dot{R}/\dot{\gamma}$. Conditions that allow isolated σ_a- and δ-type porphyroclast systems to be used as sense of vorticity indicators are: the systems should have a monoclinic shape symmetry; matrix grain size should be small with respect to porphyroclast size; matrix fabric should be homogeneous; deformation history should be simple, and observations should be made on sections normal to the inferred bulk vorticity vector for the mylonite.

INTRODUCTION

MANY deformed rocks contain megacrysts bordered by pressure shadow domains that contain material with a fabric and composition different from the matrix. Well-known examples of such megacryst systems are quartz fringes around pyrite crystals (e.g. Durney & Ramsay 1973) and adjacent to garnets in metapelites (e.g. Rosenfeld 1970, Schoneveld 1977). The geometry of such systems commonly stores information on aspects of the deformation history of the rock that are not preserved elsewhere in the fabric. In mylonitic rocks, porphyroclasts of feldspar and other relatively strong minerals are commonly preserved in a finer-grained recrystallized matrix. A specific class of megacryst system comprises porphyroclasts that show flattened mantles and tails of either dynamically recrystallized material (compositionally identical to the host grain) or reaction-softened material (for example, the reaction feldspar to white mica and quartz), the tails being derived from an originally larger clast by grain size reduction. The interpretation of such *porphyroclast systems* in the study of flow patterns in rocks has been hampered by their often highly variable shape. In our initial attempts to resolve the controversy surrounding the usefulness of porphyroclast systems we found that, even within the same thin section, apparently conflicting geometries could occur. These observations led to a reappraisal of the geometry and some aspects of the kinematics of porphyroclast systems, the results of which are presented in this paper.

The internal, three-dimensional shape symmetry of megacryst systems is usually orthorhombic or monoclinic (Figs. 1a & b). The external symmetry, or orientation of the megacryst system with respect to other fabric elements in the rock such as foliations, may also be orthorhombic or monoclinic (Fig. 1b). To determine the internal and external symmetry class, a reference plane is first defined that contains the symmetry axis of the megacryst system (x_3) and its normal (x_1) parallel to the relatively planar trace of the tail outside the complex deformation domain bordering the central megacryst

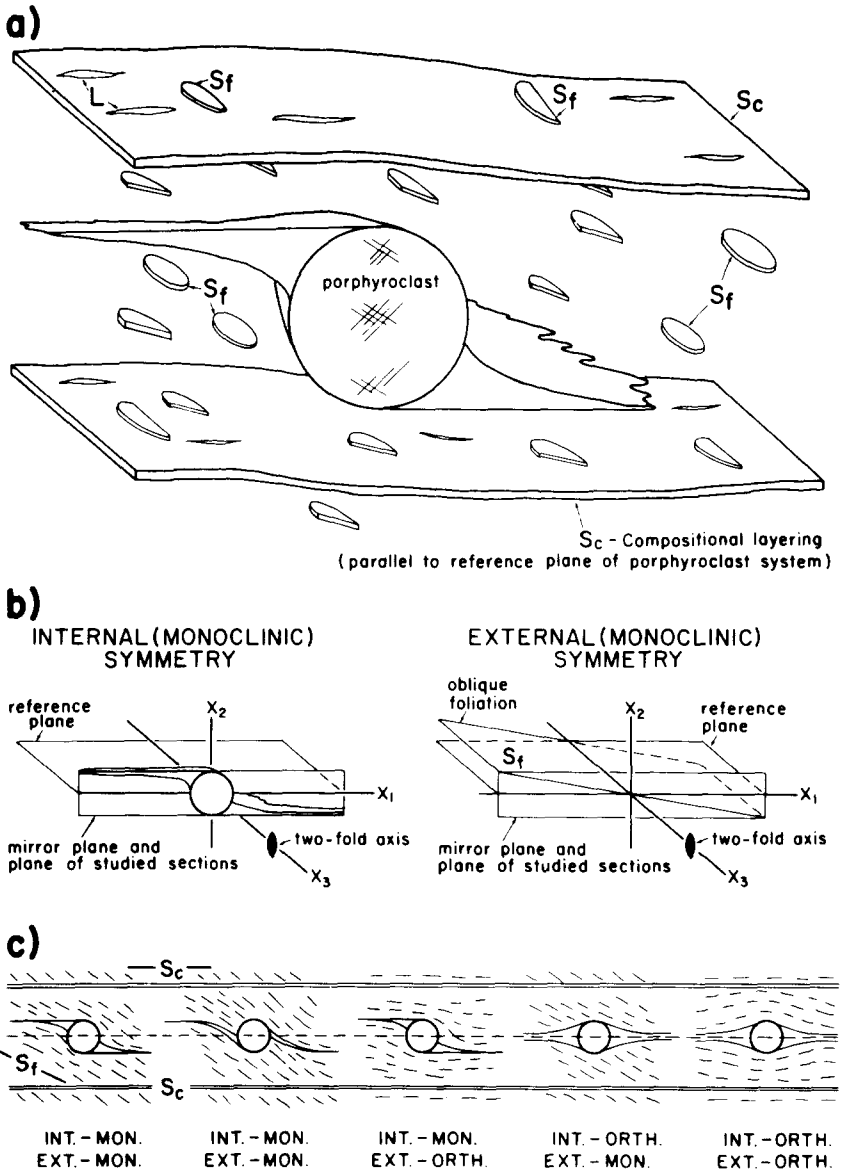

Fig. 1. (a) Geometry of a porphyroclast system in mylonitic matrix. Sinistral sense of vorticity. S_c, compositional layering; S_f, foliation defined by elongated grains; L, mineral stretching lineation. (b) Internal and external monoclinic symmetry elements. (c) Sections through porphyroclast systems normal to x_3 showing possible combinations of internal (INT.) and external (EXT.) monoclinic (MON.) and orthorhombic (ORTH.) symmetry classes. Internal and external symmetry axes coincide.

(Figs. 1b & c). If compositional layering (S_c) is present in the rock it is usually parallel to the reference plane x_1-x_3. Internal and external symmetry classes may not always coincide but symmetry axes usually do. This paper is mainly concerned with internal symmetry elements.

Experimental data and the study of naturally deformed rocks show that a monoclinic internal symmetry of megacryst systems may reflect a non-coaxial flow regime (Ghosh & Ramberg 1976, Schoneveld 1979). Porphyroclast systems in mylonitic rocks often have an internal monoclinic shape symmetry, with the symmetry axis (x_3) in the plane of the main foliation and normal to the stretching lineation, which is parallel to x_1 (Figs. 1a & b). An identical vergence of monoclinic symmetry for most porphyroclasts in a given sample suggests that the matrix was deformed by non-coaxial relatively homogeneous flow during at least some stage of the deformation history. The mylonite may have a relatively simple deformation history with little change in orientation of the kinematic framework with time, such as a single event or overprinting of events with a similar orientation of kinematic framework. In this case the symmetry pattern of the porphyroclast system can be used to obtain reliable data on the axes of the strain-rate tensor and the sense of vorticity (Lister & Price 1978, Malavieille *et al.* 1982, Passchier 1982, Simpson & Schmid 1983, Lister & Snoke 1984, Passchier 1986). Alternatively, the kinematic framework may have changed orientation with time, but some stages of deformation produced much stronger monoclinic fabric elements than others. In this case, separation of fabric elements formed during the different events is necessary, and reliable interpretations are not always possible.

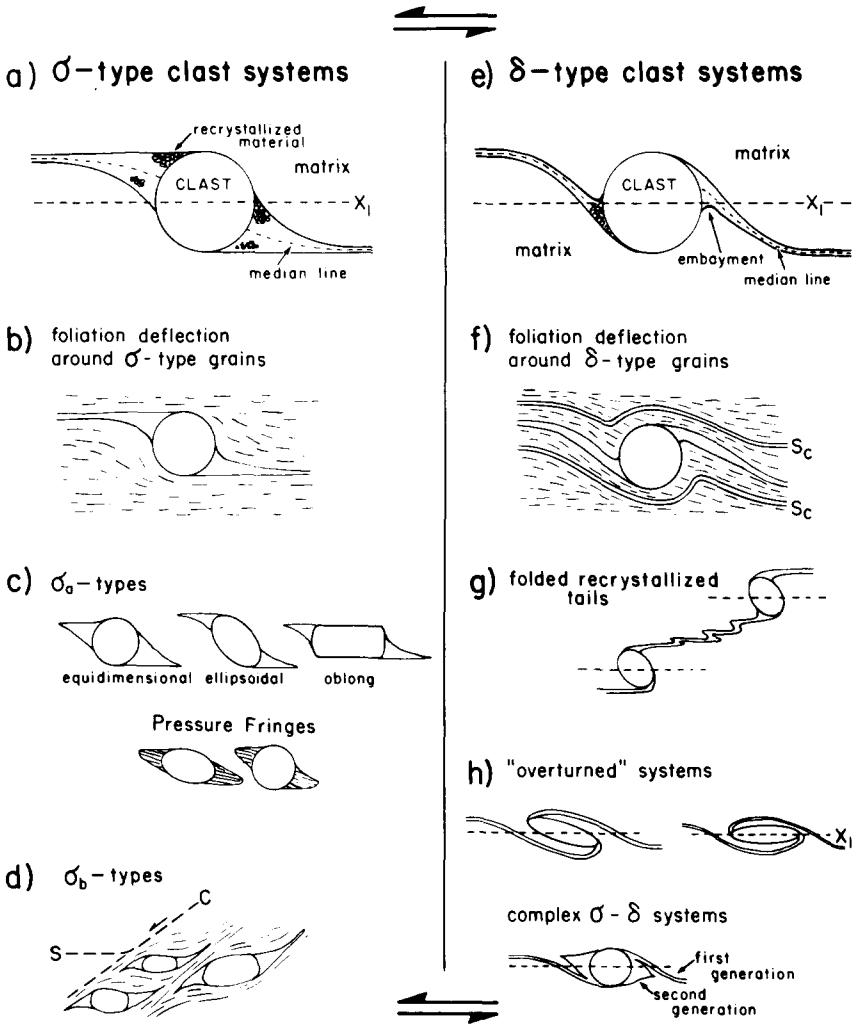

Fig. 2. Classification of porphyroclast systems with sinistral sense of vorticity. (a) σ-Type system. (b) Foliation deflection around σ-type systems. (c) σ_a-Type (equidimensional, ellipsoidal, oblong); pressure fringes. (d) σ_b-Type in S–C mylonites. (e) δ-type system. (f) Foliation deflection around δ-type systems. S_c, compositional layering. (g) Folded recrystallized tails. (h) Complex and overturned δ-type systems.

The examples presented in this paper were chosen from shear zones with apparent simple deformation histories covering a wide variety of rocks types and localities (see Appendix) in order to demonstrate the general applicability of our findings. Samples from the shear zones studied contain one dominant stretching lineation and a main foliation (S_c in Fig. 1) usually defined by both compositional layering and a subparallel mica preferred orientation. Other fabric elements that occur in many samples include oblique mica fabrics or quartz grain-shape fabrics (S_f in Fig. 1) (Simpson & Schmid 1983, Lister & Snoke 1984) and shear-band foliations of various types such as the S–C foliations of Berthé *et al.* (1979), Lister & Snoke (1984) and extensional crenulation cleavages of Platt & Vissers (1980), Platt (1984). Intersection lineations are usually perpendicular to the stretching lineation and parallel to both internal and external symmetry axes of porphyroclast systems (x_3 on Fig. 1b). For maximum information on sense of vorticity, all thin sections were cut perpendicular to x_3 (Fig. 1b). Sense of vorticity was independently determined for each sample by the use of various external markers such as deflected layering and foliation over the zone, and internal markers such as mica fish (Eisbacher 1970), shear-band foliations and oblique foliations (Simpson & Schmid 1983).

CLASSIFICATION OF PORPHYROCLAST SYSTEMS

In sections normal to the internal symmetry axis, many porphyroclast systems have a monoclinic symmetry element defined by the position of the tails with respect to the reference plane. The tails on either side of the clast 'step up' to the opposite side of this plane somewhere near the central porphyroclast (Figs. 1b and 2). This *stair-stepping* symmetry (Lister & Snoke 1984) is not affected by the way the tails are attached to the porphyroclast (Figs. 1c and 2). Porphyroclast systems can be subdivided on geometrical grounds into two main groups which have been labelled σ- and δ-type (Fig. 2). We have avoided the use of 'S–Z' descriptive terminology because of a possible unwanted reference to fold geometry.

σ-TYPE PORPHYROCLAST SYSTEM

This type, described by Simpson (1981) and Simpson & Schmid (1983) occurs in many mylonite zones on a micrometre to centimetre scale. It is characterized by wedge-shaped tails of recrystallized material with an internal monoclinic stair-stepping symmetry. The median lines of the recrystallized tails lie on opposite sides of the reference plane, even at their contact points with the central clast (Figs. 2a and 3). In some cases, another internal monoclinic symmetry element is defined by the shape of the tails; planar on the side farthest from the reference plane and concave towards the matrix on the side nearest the reference plane (Figs. 2a and 3a–e). According to Simpson & Schmid (1983), the position of the concave contacts can be used to determine the sense of vorticity if the stair-stepping internal symmetry is obscured, for example, if tails are short and a reference plane is difficult to define (Fig. 4b). σ-Type porphyroclast systems can be subdivided as follows.

σ_a-Type

These are porphyroclast sytems in which the porphyroclast lies isolated in a homogeneous matrix. Usually, the main foliation has a uniform orientation except in a small distorted zone adjacent to the porphyroclast (Figs. 2b and 3c & d) where the foliation gradually changes in orientation to become roughly parallel to the porphyroclast margins. If the recrystallized tails are long, stair-stepping is easily detectable and tails trend subparallel to the main foliation in the rock (Figs. 3e & f and 4a). This fabric is strongly reminiscent of 'Type II *S–C* mylonitic fabrics' described by Lister & Snoke (1984), and the mica fish described by them can be regarded as a special kind of σ_a-type porphyroclast system. σ_a-Type porphyroclast systems consist of weakly anisotropic minerals such as feldspar, hornblende or apatite, and their recrystallized tails are usually equigranular and structureless. In some cases, the recrystallized grains are elongate parallel to the median line of the tails (Fig. 3b). Feldspar and hornblende systems commonly show some change in composition from clast to recrystallized material and growth of some white mica and/or biotite in the tails (Figs. 3c–f). Such mica growth occurs especially under low-grade metamorphic conditions. The new micas tend to form in beard-like clusters parallel to the median line of the tails. In some cases, porphyroclasts remain rigid and are unaffected by flow in the matrix but beards of mica, quartz or calcite develop with a geometry similar to σ-type tails (Fig. 2c). Such pressure-shadow or pressure-fringe structures are not treated further in this paper because the kinematics of their formation (Malavieille *et al.* 1982) can differ significantly from the model presented here.

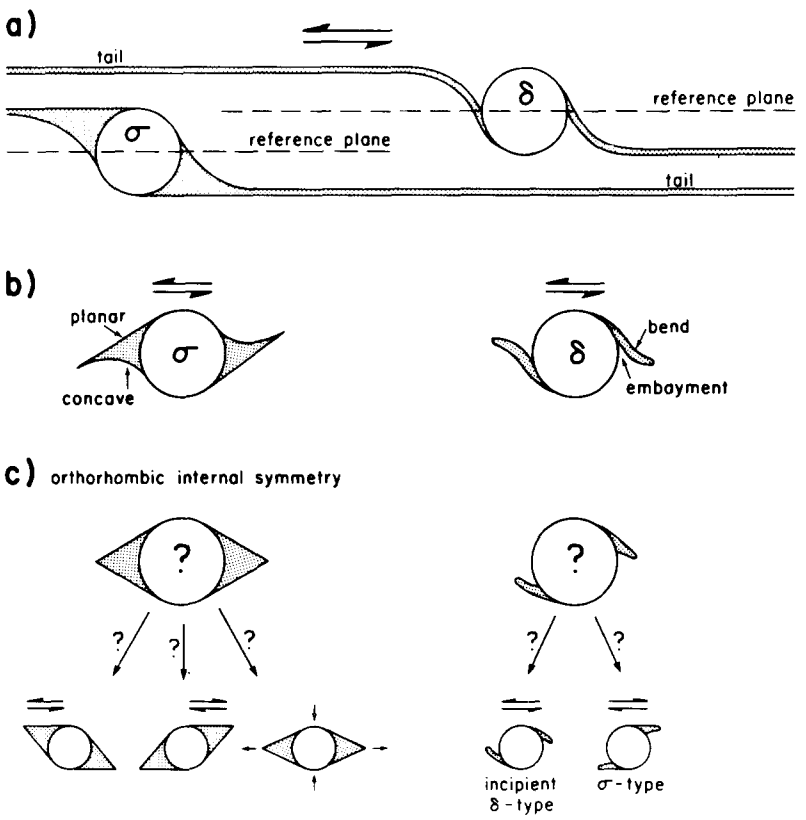

Fig. 4. Limits of the method. (a) Tails of porphyroclast systems stretch far away from central clasts. Types can be distinguished, reference planes drawn and sense of vorticity determined from stair stepping of tails and other internal symmetry markers. (b) Tails are short, no reference plane can be drawn, no stair stepping of tails occurs but other internal monoclinic symmetry elements allow types to be distinguished and sense of vorticity can usually be determined. (c) Tails are very short and types cannot be distinguished. Sense of vorticity can only be found with help of external symmetry elements.

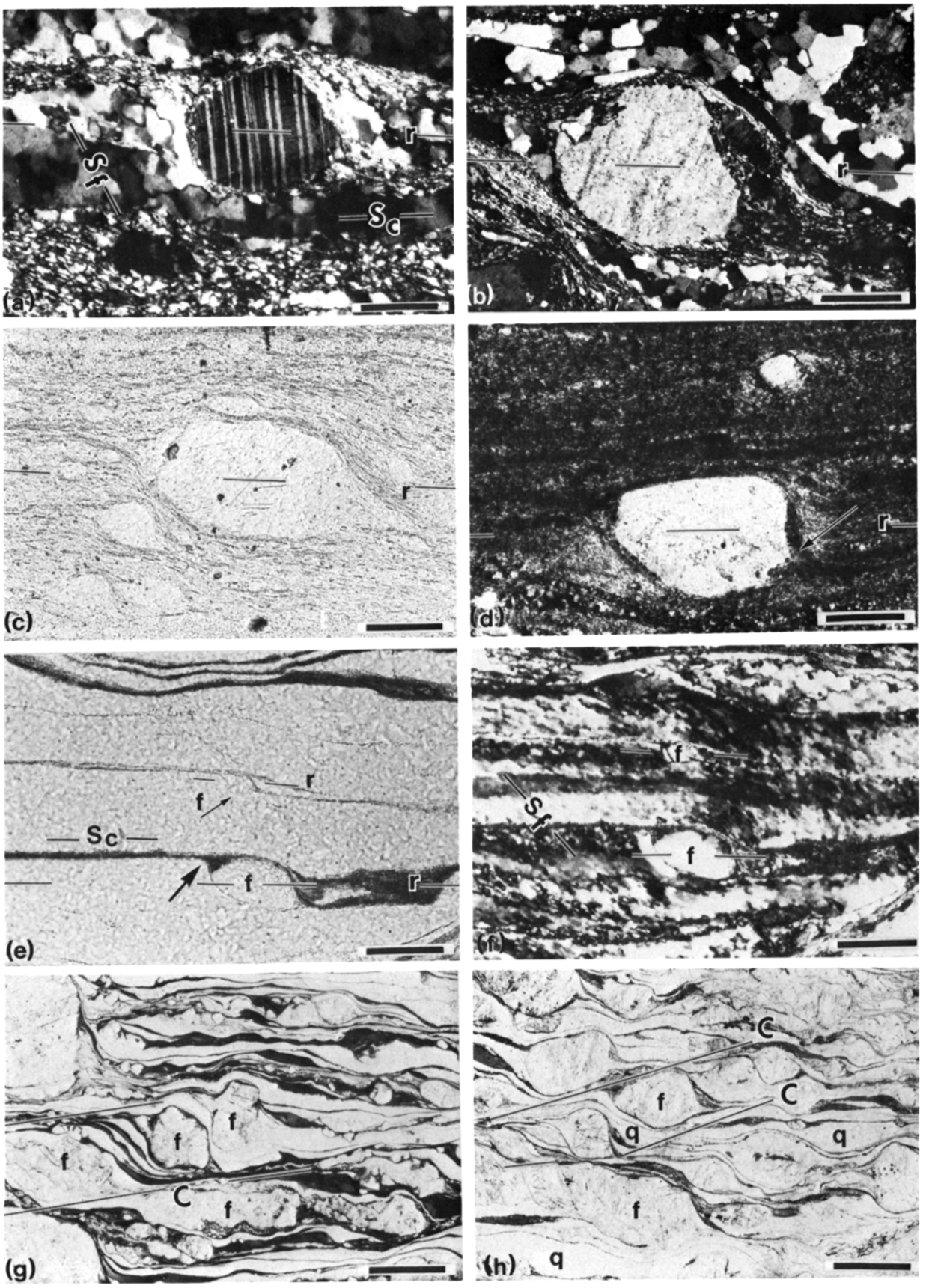

Fig. 3. σ-Type feldspar porphyroclast systems in Santa Rosa mylonite, California (details of deformation conditions in Appendix). All samples show sinistral sense of vorticity. Reference plane (r) is parallel to straight part of tails away from central clast. (a) σ_a clast with dynamically recrystallized tails in quartz-rich matrix. S_c, compositional layering; S_f, oblique quartz grain-shape foliation. (b) K feldspar σ_a clast in quartz–mica matrix. Note elongate recrystallized grains in clast tails. (c) σ_a clasts in quartz–mica matrix, plane light. Reaction of feldspar to white mica in tails. (d) σ_a clast in ultramylonite quartz–mica matrix, crossed polars. Note alteration to mica in tails and concave contact of tail with matrix (arrow). (e) σ_a feldspar clasts (**f**) in quartz-rich mylonite (plane light). Note concave contacts with matrix (large arrow) and presence of biotite (dark) in tails. (f) Same view as (e) with polars crossed to show strong oblique quartz grain-shape foliation, S_f. (g) σ_b feldspar clasts (**f**) in *S–C* mylonite (plane light). Quartz (white) and biotite (dark) ribbons define two foliations. (h) σ_b feldspar clasts (**f**) in *S–C* mylonite (plane light). Quartz (**q**) and mica ribbons define two foliations. Scale bars for (a), (c), (d), (e), (f) =150 μm; (b) = 300 μm; (g), (h) = 1500 μm.

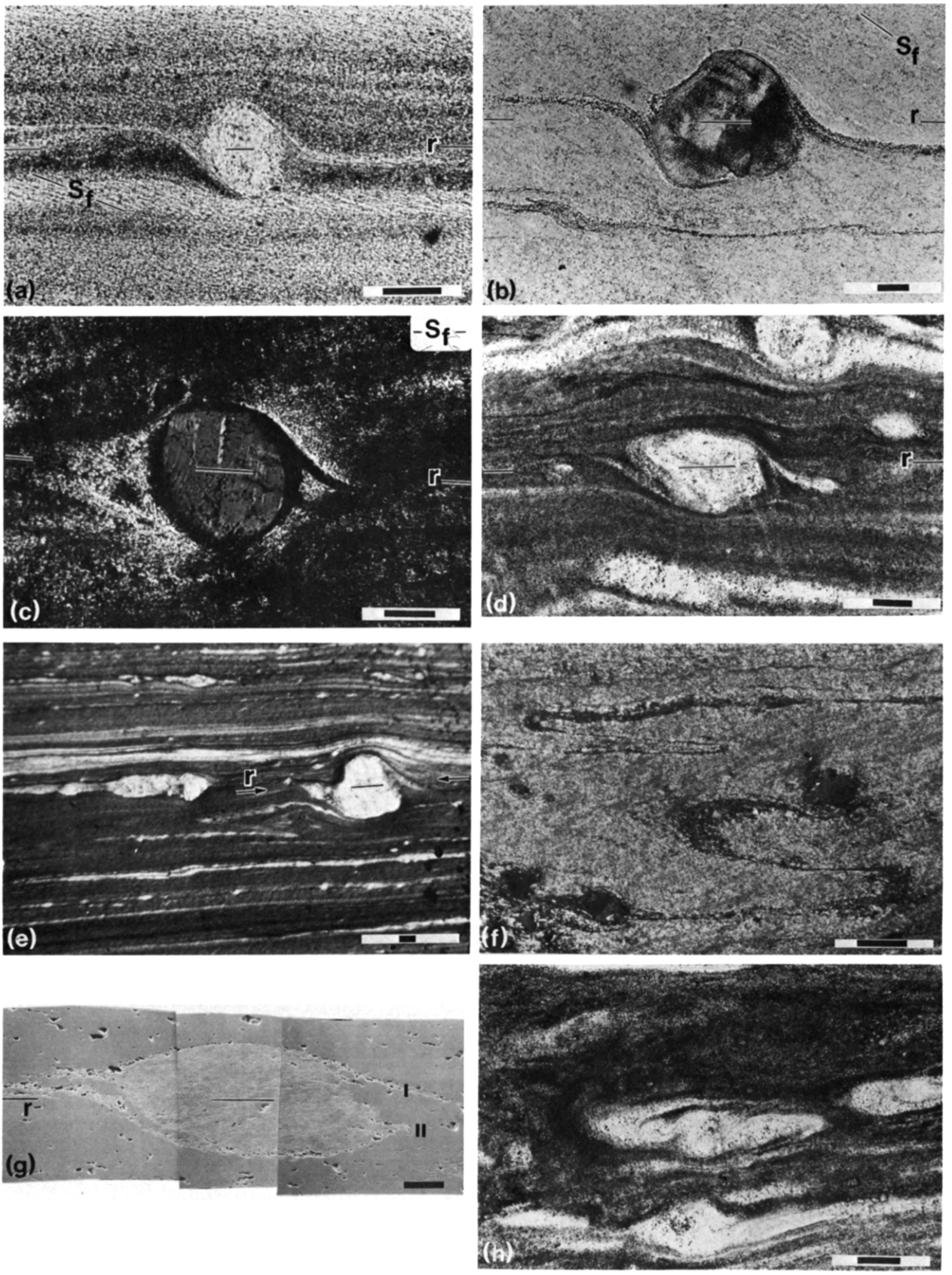

Fig. 6. δ-Type feldspar porphyroclast systems in Saint Barthélémy mylonite, French Pyrenees (details of deformation conditions in Appendix). All samples show sinistral sense of vorticity. Reference plane (**r**) indicated by solid lines. (a) δ-Type system in ultramylonite, plane light. S_f-oblique white mica foliation in quartz–feldspar band. (b) Plagioclase porphyroclast systems in dynamically recrystallized quartzite mylonite, plane light. Large δ-type clast is flanked by incipient second generation tails in quartzite embayments. Small elongate σ_a-type clast lies at lower left. S_f: oblique foliation defined by elongated quartz grains. (c) Incomplete K-feldspar δ-type system in ultramylonite with a dark mantle of recrystallized grains, crossed polars. Biotite foliation (S_f) in matrix is parallel to one polar causing general extinction except where foliation is deflected around clast system. (d) δ-Type system in ultramylonite with elongated central clast: thinning of right-hand tail towards the clast may be due to pulsating angular velocity of clast. (e) δ-Type system in ultramylonite, plane light. Compositional layering below clast is tightly folded with an opposite stair-stepping vergence to that of porphyroclast tails. (f) Folded recrystallized feldspar tails in ultramylonite, plane light. (g) SEM picture of complex plagioclase porphyroclast system in mylonitized quartzite with first (I) and second (II) generation tails. (h) Overturned porphyroclast systems in ultramylonite, plane light. Scale bars for (a), (c), (f), (g) 50 μm; (b), (d), (e), (h) 100 μm.

Many σ_a-type porphyroclast systems have an ellipsoidal central grain. Where such clasts are elongate in sections normal to x_3, their shortest dimension is usually steeply inclined to the main foliation plane with a symmetry as in Figs. 2(c) and 3(c–e). The geometry of the recrystallized tails is usually identical to that around spherical porphyroclasts.

σ_b-*Type*

Some mylonites have a heterogeneous fabric due to development of shear-band foliations. In such mylonites, σ_b-type porphyroclast systems are associated with *C*-planes (Fig. 2d) (Berthé *et al.* 1979), that is, narrow zones of high shear strain oblique to the main foliation (*S*-planes), which either predates the *C*-planes or developed synchronously. Shear-band foliations seem to present a specific type of flow partitioning in which *S*-planes undergo longitudinal extension during *C*-plane development (Platt & Vissers 1980, Platt 1984). *S*–*C* intersection lines are usually subperpendicular to the stretching lineation in the mylonite.

Several mechanisms for the development of shear-band foliations have been proposed, depending on the relative age of *S*- and *C*-planes and their orientation with respect to shear-zone boundaries and bulk incremental stretching axes (Berthé *et al.* 1979, Platt & Vissers 1980, Vernon *et al.* 1983, Lister & Snoke 1984, Platt 1984). In all types with a single set of *C*-planes, however, a consistent vergence of *S*–*C* planes is seen in sections normal to their intersection line, and the deflection of the *S*-planes as they approach the *C*-planes is always such as to decrease the acute angle between the two (Fig. 2d).

In quartz–feldspar mylonites the *S*-planes are generally defined by a subparallel alignment of quartz ribbons, feldspar porphyroclast aggregates and mica (001) planes. *C*-planes are defined by reoriented quartz ribbons and domains of recrystallized mica and feldspar (Figs. 3g & h and 5). In such mylonites the *C*-planes tend to enclose large porphyroclasts of feldspar, and dynamically recrystallized material from the feldspar grain mantle is deflected along them (Fig. 5). The resultant porphyroclast system constitutes a distinct σ-type, although individual porphyroclasts are rather less regular than those in a homogeneous matrix (Figs. 2d and 3g & h). Porphyroclasts within the σ_b-systems commonly have flat faces along the *C*-planes (Fig. 3h) and tend to occur in clusters. Within relatively wide zones of high strain along *C*-planes it is not uncommon to find σ_a-type or orthorhombic porphyroclast systems.

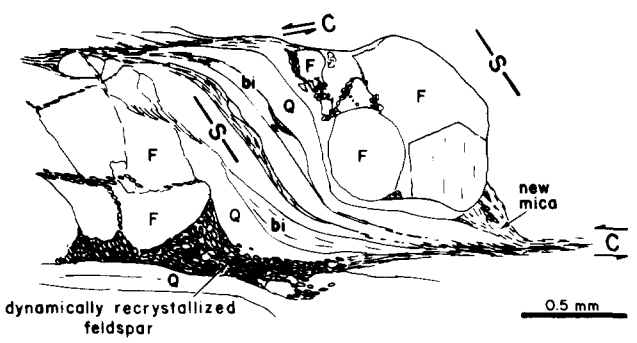

Fig. 5. Sketch from portion of Fig. 3(g) to show angular relationship among *S*- and *C*-planes and feldspar σ_b clasts (F) in a quartz (Q) and biotite (bi) matrix. Dynamically recrystallized feldspar and new mica grains are elongate parallel to median line of tails.

The recrystallized tails of σ_b-type grains may, like σ_a-type systems, differ in composition from the parent clast; and especially under low grade metamorphic conditions, they may contain a significant percentage of micas aligned subparallel to the *C*-planes. In some medium- to high-grade mylonites, elongate new feldspar grains within the recrystallized tails of σ_b-type systems define a foliation subparallel to the median line of the tail (Fig. 5).

δ-TYPE PORPHYROCLAST SYSTEMS

This type of porphyroclast system has been recognized on a micrometre to centimetre scale for feldspar in quartz–plagioclase–biotite–white mica ultramylonite from the Pyrenees (Passchier 1982), quartz–plagioclase–hornblende–biotite–epidote–muscovite ultramylonite along the Vincent thrust, California (Simpson unpublished data), quartzo-feldspathic mylonites from the Grenville Province, Canada (Davidson *et al.* 1982, Hanmer 1984) and Mt. Isa inlier, Queensland (Passchier, unpublished data). It has also been produced experimentally in sheared limestone–halite aggregates (Jordan, in press). δ-Type systems differ from σ-type systems in that the median lines of recrystallized tails cross the reference plane adjacent to the porphyroclast (Figs. 2e and 6a–d). The tails thicken more gradually towards the central clast than in σ_a-type systems (Figs. 2e & f) and consequently embayments of matrix material occur adjacent to the porphyroclast as shown in Figs. 2(e) and 6(a & b). The tails thus have distinct bends where they straighten out away from the central clast. These bends are an internal symmetry element independent of stair-stepping of the tails (Figs. 4a & b). δ-Type systems only occur around equidimensional or very slightly elongate porphyroclasts. The tails of δ-type feldspar porphyroclasts consist of equigranular recrystallized feldspar, commonly with a different chemical composition from the host porphyroclast. If a mica-preferred orientation is present in the matrix, it is deflected around the porphyroclast as shown in Figs. 2(f) and 6(a). The compositional layering can be oblique to a mica preferred orientation in the embayments, even if both foliations are parallel elsewhere in the rock (Fig. 2f). Stair-stepping symmetry is identical for σ- and δ-type systems for a particular sense of vorticity (Fig. 4a).

Folded porphyroclast systems

Porphyroclasts sometimes occur in the cores of buckle folds and sheath folds in the compositional layering of

mylonites; the disturbed flow pattern around such clasts may initiate flow instabilities which can amplify into a fold as suggested by Lister & Williams (1983) and Platt (1983). Isolated δ-type porphyroclast systems as defined above are not identical with such folded porphyroclast systems (compare Figs. 2e & g). For flow regimes approaching simple shear the systems can be distinguished by the position of the recrystallized tails with respect to the reference plane; for a particular sense of vorticity the 'stair-stepping' symmetry of δ-type (and σ-type) porphyroclast systems is *opposite* to the position of microfold limbs (Figs. 2e & g and 6e & f).

Complex and overturned porphyroclast systems

Complex porphyroclast systems with monoclinic shape symmetry resembling the normal δ-type occur in some mylonites and augen gneisses (Fig. 2h). These complex systems contain more than one set of tails (Figs. 6b & g). Overturned porphyroclast systems are characterized by tails which spiral around a commonly elongate central porphyroclast (Fig. 6h).

LIMITS OF THE METHOD

In some cases tails of porphyroclast systems can be so short that they cannot be traced outside the complexly deformed domain adjacent to the central clast (Figs. 4b & c). This means that no reference plane can be drawn and that stair-stepping internal symmetry cannot be recognized. Although other internal symmetry elements such as flat-concave pairs of tails for σ-type, and bent tails for δ-type, may still be used in these cases (Fig. 4b), errors can easily be made and external symmetry elements are needed. We would like to stress that the method of using porphyroclast systems as sense of vorticity markers as presented above is only reliable if a reference plane can be drawn.

DEVELOPMENT OF PORPHYROCLAST SYSTEMS

Non-coaxial flow in a continuum surrounding an isolated rigid object causes a spinning motion of this object with respect to the instantaneous stretching axes of the bulk flow (Ghosh & Ramberg 1976, Freeman 1985). Flow in the matrix may produce foliation elements which interfere in a complex way with the rotating object. The resulting structure contains information on the flow regime and the deformation path in a volume of material surrounding the object. 'Snowball' garnets and other porphyroblasts that grow synkinematically have received relatively more attention in the literature than have rigid porphyroclasts which decrease in size during ductile flow. The flow of material around such porphyroclasts creates internal opposite and balancing shear stresses, which are largest in the rim of the grain. Enough strain energy can be concentrated in the rim of the clasts to cause localized dynamic recrystallization and thus create a mantle of small new grains (White 1976). The volume of this mantle will tend to grow continuously at the expense of the host grain. If the aggregate of new grains is softer than the parent porphyroclast, its shape will change under the influence of flow in the matrix. Some aspects of this shape-change in non-coaxial flow will now be discussed.

The distribution of displacement paths of material points in a homogeneous continuum around spherical and ellipsoidal rigid objects in viscous simple shear flow are relatively well understood (Jeffery 1923, Bretherton 1962). The kinematics of the porphyroclast systems described above, however, are relatively complex for the following reasons: (1) the matrix is crystalline and commonly anisotropic; (2) a contrast in flow behaviour exists in many cases between the matrix and the recrystallized tails of the porphyroclast system and (3) flow is non-coaxial but rarely a simple shear throughout the deformation history. An additional uncertainty is the distribution of the recrystallization velocity at different points in the rim of the porphyroclast, which will be a function of local shear stress magnitude and the local orientation of the crystal lattice in the stress field. The shape of the recrystallized domain, and eventually of the porphyroclast system as a whole, depends on this velocity distribution and the way in which the spinning motion of the clast redistributes the newly recrystallized grains over the tails.

SHEAR BOX EXPERIMENTS

As a first, simple approximation of a developing isolated σ_a- or δ-type porphyroclast system in a shear zone, it is useful to consider the pattern of two-dimensional heterogeneous ductile flow around a rigid circular object in a homogeneous matrix deforming by simple shear. For this purpose, shear box experiments were carried out by one of us (CWP) using a 3 cm thick slab of viscous silicone putty and a 3 cm high rigid cylinder embedded within it and oriented parallel to the vorticity vector of simple shear (Fig. 7a) (Schoneveld 1979, p. 56). Only the two-dimensional flow of material points on the surface of the sample in the plane normal to the vorticity vector was studied. Figures 7(b & c) show the deformation of a square marker grid, and the pattern of displacement vectors respectively, around the cylinder for a shear strain of 0.7. The centre of the cylinder is chosen as the origin of a reference frame with the u and w axes parallel to the plane of simple shear. The angular velocity of the cylinder in radians per second was found to approach half the shear strain rate in all experiments, as predicted by theory (Jeffery 1923). In Figs. 7(b & c) the most obvious deviations from a simple shear flow pattern are (1) deflection of flow lines from planar surfaces to double monoclines around the cylinder for a distance up to one cylinder radius, (2) immediately adjacent to the cylinder surface there is an enhanced incremental shear strain near the vw plane and (3) also adjacent to the cylinder surface there is initiation of

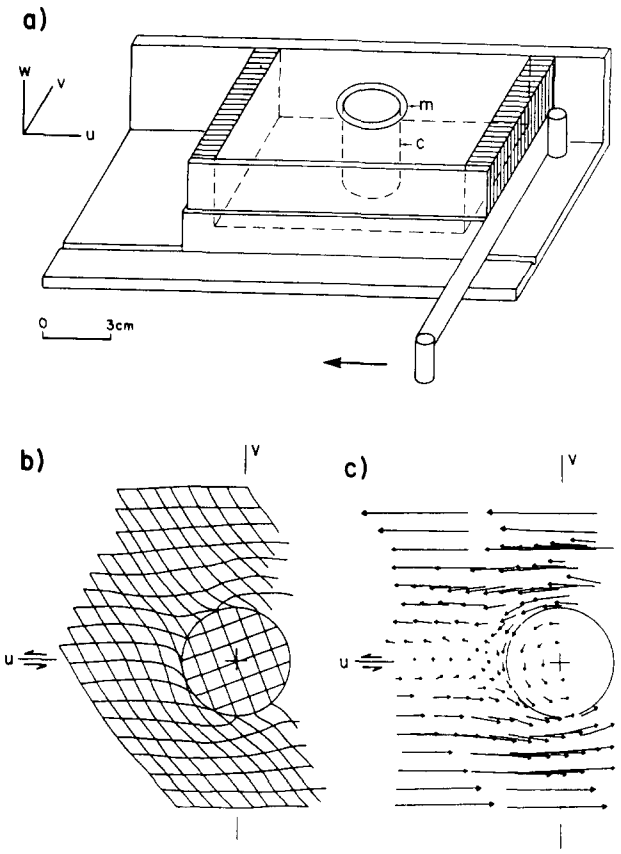

Fig. 7. (a) Schematic drawing of shear box used in the experiments. C, 3 cm high rigid cylinder; m, marker on surface of silicone putty slab. (b) Distortion of square marker grid around rigid cylinder. (c) Distribution of displacement vectors for material points around rigid cylinder. (b) and (c) at shear strain $\gamma = 0.7$. reference frame *uvw* is the same for (a), (b) and (c).

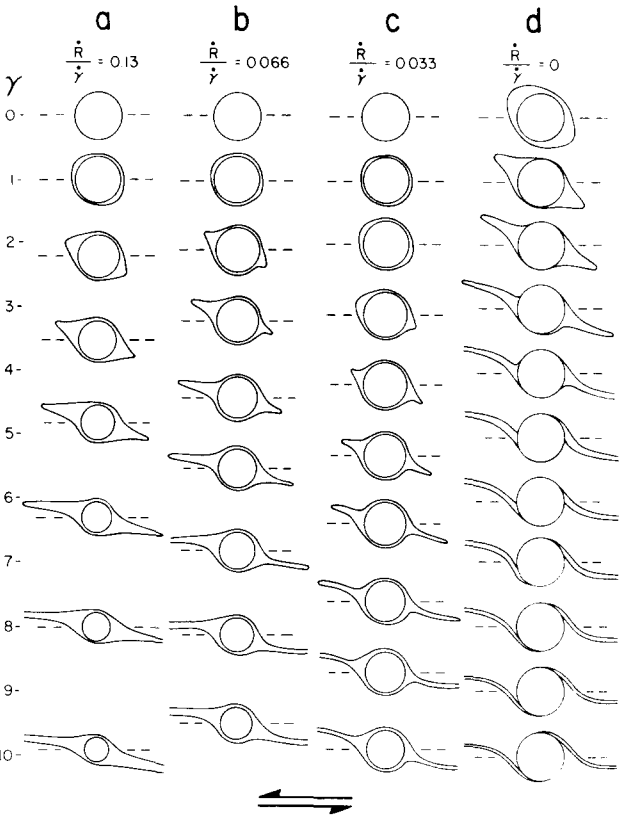

Fig. 8. Results of shear box experiments at different $\dot{R}/\dot{\gamma}$ values. $\dot{R}$, recrystallization rate; $\dot{\gamma}$, shear strain rate. Marker plane (dashed line), parallel to 'neutral surface' of simple shear. (a) $\dot{R}/\dot{\gamma} = 0.13$. (b) $\dot{R}/\dot{\gamma} = 0.066$. (c) $\dot{R}/\dot{\gamma} = 0.033$. (d) $\dot{R}/\dot{\gamma} = 0$. Shear strain (γ) increases down each column. Cylinder diameter decreases with increase in γ for (a), (b) and (c). Cylinder diameter held constant with increase in γ in (d).

minor flow crossing the *uw* plane. These three 'drag' effects are caused by the contrast, in magnitude and orientation, of displacement vectors in the rim of the rigid object and those in the adjacent matrix. Material points in the matrix pass the *v*-axis at a velocity up to twice that of adjacent points in the rim of the cylinder. In the case of homogeneous simple shear flow, a set of immobile particles would form a 'neutral surface' along the *uw* plane, but this pattern becomes disturbed adjacent to the rotating cylinder. Some aspects of these and other complex flow patterns have been discussed by Jeffery (1923) and Bretherton (1962).

A model for recrystallizing clasts

The behaviour of an isolated, rigid clast with a synkinematically recrystallized mantle in a ductilely deforming medium was modelled by the change in shape of a marker circle around rigid cylinders in shear box experiments. Although a maximum shear strain of 2 was obtainable in each experiment in the shear box, it was possible to model much higher strains by taking the end result of the previous deformation step as the initial configuration at the start of a new experiment. A series of rigid cylinders was used with diameters ranging from 15 to 31 mm in steps of 1 mm. At regular intervals during progressive simple shear the experiment was stopped and the outline of the deformed marker circle transferred onto a clear plastic sheet. The cylinder was then replaced by the next smallest one, the shear box refilled with fresh silicone putty and the outline of the previously deformed marker circle transferred onto the fresh putty surface so that the centre coincided with that of the smaller cylinder (Figs. 7a and 8). This process was then repeated several times up to a maximum shear strain of 10. Since the surface bounded by the deforming marker remained constant in area, the experiment served to model synkinematic recrystallization where the recrystallized material has rheological properties identical to the matrix.

Recrystallization in the rim of porphyroclasts is thought to result mainly from shear stresses set up by the velocity gradients between the clast and the flowing matrix. The size of these velocity gradients at any point in the rim is a linear function of the bulk shear strain rate and the diameter of the clast; a decreasing clast diameter at constant shear strain rate results in a decrease in shear stress magnitudes in the rim, and thus in lower recrystallization rates. This effect was added in the experiments by a systematic increase in the amount of incremental shear strain with each smaller cylinder replacement. In this way a constant recrystallization rate per shear strain rate ($\dot{R}/\dot{\gamma}$) could be modelled, where $\dot{R}$ is defined as the change of cylinder diameter per unit time. Finally, an

attempt was also made to model the change in shape of the recrystallized volume of material at constant shear strain rate but with varying recrystallization rates. This was done by varying the increments of shear strain between replacement of cylinders.

Results

Figure 8 shows the results of the recrystallization modelling experiments for different values of $\dot{R}/\dot{\gamma}$. The indicated marker plane (uw) coincides with the 'neutral surface' of bulk simple shear and is not identical with the reference plane x_1-x_2 for natural porphyroclast systems discussed in the first half of this paper. Only at very high finite shear strains will the two planes become subparallel. In all cases tails develop in the incremental extension quadrants of simple shear. These tails gradually become stretched subparallel to the 'neutral surface' of simple shear (uw) at a distance of half a clast diameter. This produces the typical 'stair-stepping' symmetry of tails common in naturally deformed rocks. At relatively high $\dot{R}/\dot{\gamma}$ values, typical σ_a-type tails develop which persist up to high shear strains and small clast diameters (columns a & b in Fig. 8). At lower $\dot{R}/\dot{\gamma}$ values, embayments appear in the tails similar to those characteristic of δ-type porphyroclast systems (Fig. 8c). If the cylinder diameter is kept unchanged (Fig. 8d), the circular or elliptical markers in the surrounding matrix rapidly deform to thin, δ-type systems similar to those found in some ultramylonites (compare Figs. 8d and 6a–d).

Considering the large differences in material properties and rigid object shape between naturally deformed porphyroclast systems and the cylinder/marker systems of the experiments, it is surprising that such a close analogy in geometry is reached. This is probably a result of the following effects. (1) The components of flow around spherical rigid objects in the w-direction, which are absent in the case of two-dimensional flow around a cylinder, apparently do not change the basic shape of a developing porphyroclast system. The flow lines of disturbed simple shear flow around a spherical object tend to describe double domes instead of monoclines as in the case of a rigid cylinder, but cross-sections parallel to the uv plane give very similar patterns of flow lines in both cases, provided these sections are taken near the centre of the rigid sphere. (2) The crystalline nature of the matrix material in naturally deformed rocks may approach the behaviour of an anisotropic continuum if the grain-size is small with respect to the porphyroclast system studied, as was the case for most of the natural samples described above. (3) The anisotropic nature of the matrix material around porphyroclast systems seems to have had little effect on the geometry of developing systems. Both σ_a- and δ-type porphyroclast systems have been found in strongly anisotropic ultramylonites and in weakly anisotropic mylonites and quartzites. (4) The contrast in flow behaviour between the matrix and the recrystallized tails seems to have been small in the samples studied. Buckle folding or boudinage of recrystallized feldspar tails is rare in mylonite and absent in most ultramylonite samples. Also, the deflection of mica foliation in ultramylonite samples is similar around porphyroclasts with and without tails (Passchier 1982). (5) The naturally deformed porphyroclast systems described above were samples from shear zones in which internal fabric elements and zone geometry were indicative of flow regimes approaching simple shear during most of their history. Small deviations from simple shear may weaken the stair-stepping symmetry of the tails, yet maintain other internal monoclinic symmetry elements of the porphyroclast systems (Fig. 4b).

THE GENESIS OF σ-TYPE VS δ-TYPE PORPHYROCLAST SYSTEMS

One of the most important factors that determines whether σ_a- or δ-type systems will develop seems to be the ratio $\dot{R}/\dot{\gamma}$. If $\dot{R}/\dot{\gamma}$ is high, the flow of recrystallized material in the tails away from the central clast is continuously supplemented by the production of new grains. This effect, and the rapidly decreasing amplitude of the double domes of flow lines around the clast due to decrease in its diameter, probably cooperate in forming the relatively straight outer boundaries to wide recrystallized tails so characteristic of σ_a-type systems. At low $\dot{R}/\dot{\gamma}$ values, tails of recrystallized material become relatively thin and are deflected by drag due to the spinning motion of the porphyroclast which is at a maximum near the marker plane. This causes the development of the characteristic embayments and bends in tails of the δ-type system. However, the actual flow pattern of material points around the porphyroclasts in both types of systems may be very similar.

A second factor of importance is the finite shear strain. Figure 8 shows that at low shear strain values most porphyroclast systems are of σ_a-type or lack monoclinic symmetry; δ-type systems only become recognizable at higher shear strains. This is confirmed for naturally deformed rocks where δ-type systems have been exclusively found in ultramylonites or mylonitic quartzites and gneisses and never in weakly deformed rocks.

A third factor influencing the development of porphyroclast systems is the shape of the central clast. This factor has not been treated in the experiments but can be deduced from naturally deformed samples. Normal δ-type systems have only been found around porphyroclasts with round or weakly elliptical cross-sections. Central clasts with more oblong shapes (length/width ratio exceeding 2) either belong to σ_a-type systems or to overturned δ-type systems as illustrated in Fig. 6(h). Most of these clasts have their long axis at a low angle to the reference plane. This is probably because ellipsoidal rigid bodies in simple shear flow rotate in a pulsating way according to:

$$\dot{\phi} = \dot{\gamma}(C^2 \cos^2\phi + \sin^2\phi)/(C^2 + 1),$$

where $\dot{\phi}$ is the angular velocity, ϕ the angle of the long

axis of the clast with the v-axis and C the clast length/width ratio. This equation applies to cases where one of the symmetry axes of the ellipsoid parallels the vorticity vector of simple shear (Jeffery 1923, Ghosh & Ramberg 1976, Freeman 1985). It is apparent from the equation that porphyroclasts with an elliptical cross-section will tend to lie with their long axes at low angles to the shear plane of simple shear for much of the deformation history, during which they rotate slowly. Since δ-type systems form due to the drag of the spinning clast on the developing tails, they will not tend to form around elongated clasts during this stage of the rotational motion. As deformation continues, oblong clasts will eventually accelerate and 'flip over' to enter a new period of slow rotation. Overturned δ-type porphyroclast systems may be the result of such an event (Figs. 6d & h). Such structures are transient and may rapidly become obscured by further deformation.

Complex porphyroclast systems

Some δ-type porphyroclast systems, especially in ultramylonites, have more than one set of recrystallized tails as illustrated in Figs. 2(h) and 6(g). These complex porphyroclast systems are sometimes symmetric but commonly have a second tail on one side only. Similar structures have been generated during some of the shear box experiments, especially at high finite strains (Fig. 9). When $\dot{R}/\dot{\gamma}$ was suddenly increased during the generation of a δ-type system, the newly created 'recrystallized' volume was not added to the existing tails but formed instead into a new, second set of tails. In naturally deformed rocks fluctuations in shear strain rate and recrystallization rate are probably responsible for the generation of many complex porphyroclast systems. Some overturned porphyroclast systems with an oblong central grain may develop into complex systems if sufficient recrystallized material can be produced during the period that the clast lies with its long axis in the direction of the shear-plane of simple shear. This may be the case for Fig. 6(g).

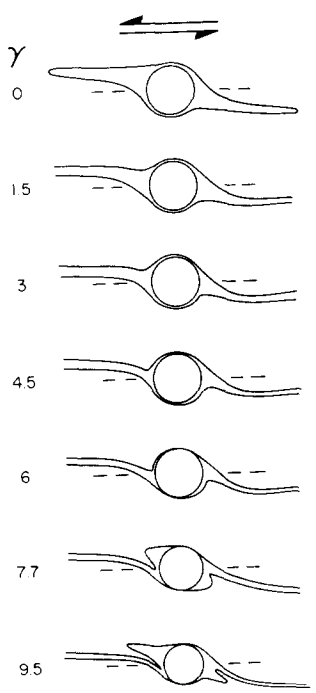

Fig. 9. Complex porphyroclast systems produced in shear box experiment, starting with a σ-type system ($\gamma = 0$). Cylinder diameter kept constant up to $\gamma = 6$. During last two stages ($\gamma = 7.7$ and $\gamma = 9.5$), cylinder diameter was suddenly decreased synkinematically. Marker plane (dashed line) is parallel to 'neutral surface' of simple shear.

σ_b-Type porphyroclast systems

These systems (Figs. 2d and 3g & h) form in a more complicated flow regime than either the σ_a- or δ-type. They are centred on lenses of relatively low finite shear strain and surrounded by shear bands in which the recrystallized tails are situated. Such structures can form by enhanced grain-size reduction in the shear bands without a significant angular velocity of the porphyroclast with respect to the bands. In an external reference frame fixed to the bulk instantaneous stretching axes of the volume of mylonite containing the systems, the porphyroclasts may in fact rotate in an opposite sense to the bulk vorticity because of rotation of the C-planes, even if they are equidimensional. It should be emphasized that to determine the bulk vorticity in σ_b-type systems it is necessary to use porphyroclast groups, such as are illustrated in Figs. 3(g & h), and not rely on individual porphyroclast geometry.

CONCLUSIONS

Isolated σ_a- and δ-type porphyroclast systems with monoclinic shape symmetry in mylonites can serve as valuable indicators of the sense of vorticity. Ideally, the following conditions should be met: (1) the grainsize of the matrix should be small with respect to the porphyroclasts; (2) the fabric in the matrix should be homogeneous; (3) the symmetry of the porphyroclast systems should be formed during one phase of deformation and should not be the result of overprinting; (4) porphyroclast tails should be long enough to allow a reference plane to be drawn and (5) observations should be made on sections normal to the main foliation and parallel to the stretching lineation; that is, normal to the inferred bulk vorticity vector of non-coaxial flow in the mylonite and the symmetry axis of the porphyroclast systems.

Sense of vorticity can be determined from: (1) the internal stair-stepping symmetry of the tails away from the central clast of either porphyroclast system (Figs. 2 and 4a) and (2) the internal symmetry elements such as concave and flat pairs of matrix-tail contacts in the case of σ_a-type systems, and bent tails and matrix embayments adjacent to the central clast of δ-type systems (Figs. 2 and 4b). Care should be taken not to confuse folded porphyroclast systems and δ-type systems since this will give erroneous results. In the samples studied, 95% of porphyroclast systems with monoclinic symmetry gave a sense of vorticity using these techniques

that was consistent with the vorticity sense as determined from independent indicators (*S–C* planes, oblique grain shape fabrics, etc.). Non-fitting systems were either irregular in shape or occurred in domains where the mylonitic fabric was strongly inhomogeneous.

The conditions which favour development of σ_a-type systems seem to be: (1) relatively high recrystallization rates at particular shear strain rates; (2) low finite strain values and (3) an oblong shape of the porphyroclast. δ-Type systems form preferentially at low recrystallization rates, large finite strain values and with equidimensional porphyroclast shape. σ_b-Type porphyroclast systems seem to form in a more complex way than either σ_a- or δ-type, but can be used as indicators of the sense of vorticity if checked against other kinematic indicators.

Acknowledgements—This work was supported in part by NSF grants EAR-8121438, EAR-8305846, EAR 8406662 and EAR-8406567 to Simpson. We thank L. Sharp for assistance with photographs, P. Sullivan and P. Hill for secretarial assistance, and S. Chiang for drafting the figures. Constructive comments by S. Hanmer, R. Tirrul, R. Wintsch and an anonymous referee are acknowledged with thanks.

REFERENCES

Anderson, J. R. 1983. Petrology of a portion of the eastern Peninsular ranges mylonite zone, southern California. *Contr. Miner. Petrol.* **84**, 253–271.

Berthé, D., Choukroune, P. & Jegouzo, P. 1979. Orthogneiss, mylonite and non-coaxial deformation of granites: the example of the South Armorican Shear-zone. *J. Struct. Geol.* **1**, 31–42.

Boullier, A-M. & Bouchez, J-L. 1978. Le quartz en rubans dans les mylonites. *Bull. Soc. géol. Fr.* **7**, 253–262.

Bretherton, F. P. 1962. The motion of rigid particles in a shear flow at low Reynolds numbers. *J. Fluid Mech.* **14**, 419–440.

Davidson, A., Culshaw, N. G. & Nadeau, L. 1982. A tectonometamorphic framework for part of the Grenville province, Parry Sound region, Ontario. *Geol. Surv. Canada, Curr. Res.* **82-1A**, 175–190.

Durney, D. W. & Ramsay, J. G. 1973. Incremental strains measured by syntectonic crystal growths. In: *Gravity and Tectonics* (edited by De Jong, K. A. & Scholten, R.). Wiley, New York, 67–96.

Eisbacher, G. H. 1970. Deformation mechanics of mylonite rocks and fractured granites in Cobequid mountains, Nova Scotia, Canada. *Bull. geol. Soc. Am.* **81**, 2009–2020.

Freeman, B. 1985. The motion of rigid ellipsoidal particles in slow flows. *Tectonophysics* **113**, 163–183.

Ghosh, S. K. & Ramberg, H. 1976. Reorientation of inclusions by combination of pure shear and simple shear. *Tectonophysics* **34**, 1–70.

Hanmer, S. K. 1984. The potential use of planar and elliptical structures as indicators of strain regime and kinematics of tectonic flow. *Geol. Surv. Canada, Curr. Res.* **84-1B**, 133–142.

Jeffery, G. B. 1923. The motion of ellipsoid particles immersed in a viscous fluid. *Proc. R. Soc. Lond.* **A102**, 161–179.

Jordan, P. G. in press. The deformational behaviour of bimineralic limestone–halite aggregates. *Tectonophysics.*

Knipe, R. J. & Wintsch, R. P. 1985. Heterogeneous deformation, foliation development and metamorphic processes in a polyphase mylonite. In: *Metamorphic Reactions: Kinetics, Textures and Deformation* (edited by Thompson, A. B. & Rubie, D. C.), 181–210.

Lister, G. S. & Price, G. P. 1978. Fabric development in a quartz–feldspar mylonite. *Tectonophysics* **49**, 37–78.

Lister, G. S. & Williams, P. F. 1983. The partitioning of deformation in flowing rock masses. *Tectonophysics* **92**, 1–33.

Lister, G. S. & Snoke, A. W. 1984. *S–C* Mylonites. *J. Struct. Geol.* **6**, 617–638.

Malavieille, J., Etchecopar, A. & Burg, J-P. 1982. Analyse de la géometrie des zones abritées: simulations et application à des éxamples naturels. *C. r. Acad. Sci. Paris* **294**, 279–284.

Passchier, C. W. 1982. Mylonitic deformation in the Saint-Barthélémy massif, French Pyrenees. GUA papers of Geology, Series 1, Vol. 16, City University of Amsterdam.

Passchier, C. W. 1983. The reliability of asymmetric *c*-axis fabrics of quartz to determine sense of vorticity. *Tectonophysics* **99**, T9–T18.

Passchier, C. W. 1984. Mylonite dominated footwall geometry in a shear zone, central Pyrenees. *Geol. Mag.* **121**, 429–436.

Passchier, C. W. 1985. Water-deficient mylonite zones—an example from the Pyrenees. *Lithos* **18**, 115–127.

Passchier, C. W. 1986. Flow in natural shear zones—the consequences of spinning flow regimes. *Earth Planet. Sci. Lett.* **77**, 70–80.

Platt, J. P. 1983. Progressive refolding in ductile shear zones. *J. Struct. Geol.* **5**, 619–622.

Platt, J. P. 1984. Secondary cleavages in ductile shear zones. *J. Struct. Geol.* **6**, 439–442.

Platt, J. P. and Vissers, R. L. M. 1980. Extensional structures in anisotropic rocks. *J. Struct. Geol.* **2**, 397–410.

Rosenfeld, J. L. 1970. Rotated garnets in metamorphic rocks. *Spec. Pap. geol. Soc. Am.* 129.

Schoneveld, C. 1977. A study of some typical inclusion patterns in strongly paracrystalline-rotated garnets. *Tectonophysics* **39**, 453–471.

Schoneveld, C. 1979. The geometry and significance of inclusion patterns in syntectonic porphyroclasts. Ph.D. thesis, Leiden.

Sharp, R. V. 1966. Ancient mylonite zone and fault displacements in the Peninsular Ranges of southern California. *Spec. Pap. geol. Soc. Am.* **101**, 333.

Simpson, C. 1981. Ductile shear zones; a mechanism of rock deformation. Ph.D. thesis, Zurich.

Simpson, C. 1984. Borrego Springs–Santa Rosa mylonite zone: a late Cretaceous west-directed thrust in southern California. *Geology* **12**, 8–11.

Simpson, C. 1985. Deformation of granitic rocks across the brittle–ductile transition. *J. Struct. Geol.* **7**, 503–511.

Simpson, C. & Schmid, S. M. 1983. An evaluation of criteria to deduce the sense of movement in sheared rocks. *Bull. geol. Soc. Am.* **94**, 1281–1288.

Theodore, T. J. 1970. Petrogenesis of mylonites of high metamorphic grade in the Peninsular ranges of southern California. *Bull. geol. Soc. Am.* **81**, 435–450.

Vernon, R. H., Williams, V. A. & D'Arcy, W. F. 1983. Grain size reduction and foliation development in a deformed granite batholith. *Tectonophysics* **92**, 123–146.

White, S. H. 1976. The effects of strain on the microstructures, fabrics and deformation mechanisms in quartzites. *Phil. Trans. R. Soc. Lond.* **A283**, 69–86.

APPENDIX: SAMPLE LOCALITIES AND DEFORMATION CONDITIONS

All photomicrographs of σ-type systems in Fig. 3 were taken from samples of the Eastern Peninsular Ranges Mylonite Zone (EPRMZ) in southern California (Sharp 1966). Cretaceous granodiorite and tonalite plutonic protoliths were deformed during the late Cretaceous at 500–650°C and <500 MPa in the presence of H_2O-rich fluids according to Anderson (1983). However, deformation conditions range from lower greenschist to upper amphibolite facies in different parts of the EPRMZ (Theodore 1970, Anderson 1983, Simpson 1984, 1985).

The quartz–K-feldspar–plagioclase (An_{28})–biotite–muscovite mylonites in Figs. 3(a & b) are from the epidote–amphibolite facies Santa Rosa section of the EPRMZ (Simpson 1985). The main foliation is defined by (1) type 3 quartz ribbons (Boullier & Bouchez 1978) containing 30–100 μm diameter recrystallized grains, (2) zones 100 to 300 μm wide of recrystallized feldspar (grain size 5–10 μm) and (3) recrystallized biotite and muscovite grains. A secondary (S_f) foliation is defined by elongate recrystallized quartz and feldspar grains. K-feldspar and plagioclase σ_a-type porphyroclast commonly have 5–10 μm-wide recrystallized rims. The recrystallized feldspar grains in clast tails tend to be elongate parallel to the median line of the tail.

Figures 3(c–h) are from the Borrego Springs section of the EPRMZ (Simpson 1985) and contain quartz–biotite–plagioclase (An_{30})–chlorite–epidote–white mica–sphene. Deformation occurred under middle greenschist conditions. The main foliation is defined by type 2 quartz ribbons (Boullier & Bouchez 1978) and kinked biotite (altering to chlorite and opaques). A second foliation (S_f) is defined by elongate recrystallized quartz grains. Figures 3(c & d) occur within narrow

(<1 cm wide) quartz-poor ultramylonite zones that contain evenly distributed, fine-grained (1–5 μm) biotite and white mica. Recrystallized mantles were not observed around the feldspar porphyroclasts in Figs. 3(c–f), and in all samples alteration of the feldspar to micaceous minerals was advanced in the clast tails. The mylonites in Figs. 3(g & h) contain a very high density of σ_b-type feldspar porphyroclasts and are thought to have had a porphyritic protolith. The σ_b-type feldspar clasts show 2–5 μm thick mantles of recrystallized grains and their tails are composed predominantly of <5 μm recrystallized feldspar grains with only very minor incorporation of micaceous minerals.

Figure 6 photomicrographs are of samples from the St. Barthélémy mylonite, Central French Pyrenees (Passchier 1982, 1983). In ultramylonite bands (6a–h) the matrix consists of biotite–plagioclase–quartz–white mica with an average grainsize of 2–5 μm. Spherical and ellipsoidal δ-type porphyroclasts of feldspar, quartz, sillimanite, zircon, monazite and apatite occur. Deformation occured at 450–550°C and 200–300 MPa in the presence of a low H_2O/high CO_2 content metamorphic fluid (Passchier 1984, 1985). Postkinematic grain growth was weak to absent (Passchier 1982). The main mylonitic foliation is defined by a compositional layering and a mica preferred orientation, subparallel to it. In many cases, beards of relatively coarse biotite have formed with a geometry similar to σ-type tails, even in some δ-type porphyroclast systems. Many feldspar porphyroclasts have grain boundaries that transect original internal zoning in the crystal. Most of the >50 μm clasts of feldspar, quartz and apatite are surrounded by mantles of fine-grained (1–5 μm) recrystallized material. Some K-feldspar grains are surrounded by a 1.5 μm thick rim of plagioclase, which suggests that limited syntectonic growth or displacement occurred (cf. Knipe & Wintsch 1985).

Figures 6(b & g) are taken from samples of a 3 cm wide mylonitized quartz lens in granodiorite of the Saint Barthélémy Massif, (Passchier, unpublished data). The lens contains narrow, straight trails of recrystallized K-feldspar in a matrix of 10–30 μm-sized dynamically recrystallized quartz grains. The new quartz grains are highly elongate and aligned with their long axis at 28° to the compositional layering. A few porphyroclasts of plagioclase and K-feldspar occur. All porphyroclasts smaller than 100 μm and larger, highly elongate clasts (up to 500 μm in length) have tails with a σ-type morphology. However, the larger spherical to slightly ellipsoidal clasts (up to 500 μm in diameter) have a δ-type morphology.